AD-A118 520 NAVAL RESEARCH LAB WASHINGTON DC F/G 20/9
HIGH POWER MICROWAVE ENERGY COUPLING TO NITROGEN DURING BREAKDO--ETC(U)
AUG 82 W M BOLLEN, C L YEE, A W ALI
UNCLASSIFIED NRL-MR-4865 NL

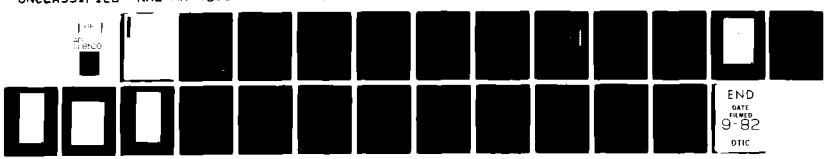

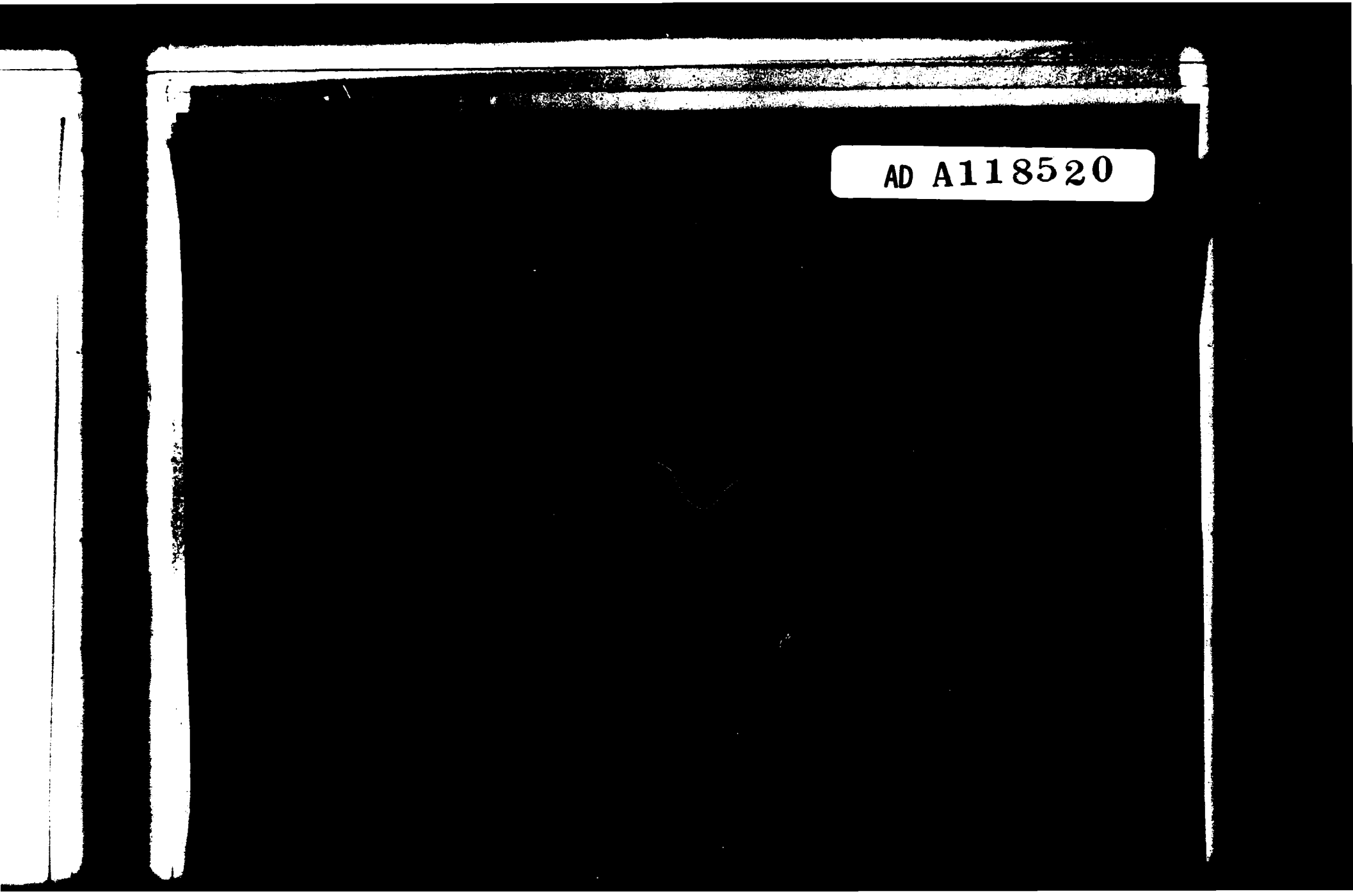

SECURITY CLASSIFICATION OF THIS PAGE (When Data Entered)

| REPORT DOCUMENTATION PAGE | | READ INSTRUCTIONS BEFORE COMPLETING FORM |
|---|---|---|
| 1. REPORT NUMBER<br>NRL Memorandum Report 4865 | 2. GOVT ACCESSION NO.<br>AD-A118520 | 3. RECIPIENT'S CATALOG NUMBER |
| 4. TITLE (and Subtitle)<br>HIGH POWER MICROWAVE ENERGY COUPLING TO NITROGEN DURING BREAKDOWN | | 5. TYPE OF REPORT & PERIOD COVERED<br>Interim report on a continuing NRL problem.<br>6. PERFORMING ORG. REPORT NUMBER |
| 7. AUTHOR(s)<br>W.M. Bollen*, C.L. Yee*, A.W. Ali, M.J. Nagurney*, and M.E. Read | | 8. CONTRACT OR GRANT NUMBER(s) |
| 9. PERFORMING ORGANIZATION NAME AND ADDRESS<br>Naval Research Laboratory<br>Washington, DC 20375 | | 10. PROGRAM ELEMENT, PROJECT, TASK AREA & WORK UNIT NUMBERS<br>NAVSEA, SF-68-344-601; 47-0868-0-2 |
| 11. CONTROLLING OFFICE NAME AND ADDRESS<br>Naval Sea Systems Command<br>Washington, DC 20362 | | 12. REPORT DATE<br>August 10, 1982<br>13. NUMBER OF PAGES<br>23 |
| 14. MONITORING AGENCY NAME & ADDRESS(if different from Controlling Office) | | 15. SECURITY CLASS. (of this report)<br>UNCLASSIFIED<br>15a. DECLASSIFICATION/DOWNGRADING SCHEDULE |

16. DISTRIBUTION STATEMENT (of this Report)

Approved for public release; distribution unlimited.

17. DISTRIBUTION STATEMENT (of the abstract entered in Block 20, if different from Report)

18. SUPPLEMENTARY NOTES

*Present address: Mission Research Corporation, Alexandria, VA 22304

19. KEY WORDS (Continue on reverse side if necessary and identify by block number)

Microwave
Breakdown
Ionization
Wave energy coupling

20. ABSTRACT (Continue on reverse side if necessary and identify by block number)

Microwave energy coupling to nitrogen for breakdown conditions have been investigated. The experiments were performed in 25 Torr nitrogen using a 35 GHz 1 μs microwave pulse focused to 33 kW/cm$^2$. The plasma created during breakdown was observed to travel towards the source with a velocity of $4.6 \times 10^6$ cm/s. Spectroscopic measurements using a nitrogen helium mixture indicate the average electron density over a 2 cm chord to be $4.4 \times 10^{12}$ cm$^{-3}$, and the electron temperature to be 3.8 eV. Microwave (Continues)

DD FORM 1 JAN 73 1473 EDITION OF 1 NOV 65 IS OBSOLETE
S/N 0102-014-6601

SECURITY CLASSIFICATION OF THIS PAGE (When Data Entered)

20. ABSTRACT (Continued)

cutoff was observed photographically and suggest the peak electron density to be collisional critical density. Computer simulations were also performed and their results are in accord with the experimental results.

CONTENTS


I. INTRODUCTION ..... 1

II. EXPERIMENT ..... 3

A. Apparatus ..... 3
B. Discussion of the Experimental Results ..... 6
1. Time Resolved Photographs of Breakdown ..... 6
2. Spectroscopic Measurement of Density and Temperature .. 12

III. COMPUTER SIMULATION ..... 14

IV. CONCLUSION ..... 19

ACKNOWLEDGMENTS ..... 19

REFERENCES ..... 20

# HIGH POWER MICROWAVE ENERGY COUPLING TO NITROGEN DURING BREAKDOWN

## I. INTRODUCTION

Microwave breakdown studies of gaseous elements have been carried out extensively over a wide range of pressures and for several microwave frequencies using CW and pulsed radiation sources[1]. The main emphasis on these studies was the determination of the breakdown power threshold, and its dependence on the gas pressure and the microwave frequency. The coupling of microwave energy into the breakdown plasma and neutral gas has not been studied in detail. The reason for this is that until recently no high power microwave sources have been available to perform such studies. Most of the early work performed on breakdown thresholds was performed using high Q cavities to obtain the necessary electric field to break down the gas. Once breakdown of the gas occurred, the Q of the cavity dropped and the interaction changed. Using the NRL high power gyrotron facility, we have been able to eliminate the need for cavities and have performed experiments using a focused geometry[2] to examine the coupling of microwave energy to nitrogen gas during breakdown. We have also modeled the experiments using a 1-D computer simulation code[3]. Simulations were performed in a spherical geometry using a self-consistent, nitrogen chemistry, wave optics, microwave breakdown simulation code, MINI.

The main emphasis of this paper is on the ionization front created during nitrogen breakdown and its motion and plasma properties as observed experimentally. This motion is not a movement of the plasma but rather a movement of where the strongest ionization of the gas is taking place. We believe it to be due to two effects: 1) delayed ionization and 2) reflection from the plasma itself. Since the electron density is proportional to $e^{tI_o}$, where $I_o$ is the local microwave intensity, breakdown occurs faster in those regions of high intensity. In a focused system this results in breakdown beginning at the focus. The breakdown

Manuscript submitted May 27, 1982.

then moves back into the lower intensity region as time progresses. If nothing else is occurring, one would then observe a cone of plasma late in time. However, the plasma is both absorptive and reflective. The reflection results in standing wave patterns. Thus peaks $\lambda/2$ apart are seen to grow in time. The first peak is $\lambda/4$ from the plasma surface. As the density increases in these peaks, they become reflective and absorptive, cutting off the microwave energy to peaks behind them. Again, the density grows as $e^{atI_o}$, and, therefore, those peaks nearest the focus initially grow fastest. If only one peak were reflecting, we would expect $\lambda/2$ structure. However, all the peaks reflect and, therefore, we expect $\lambda/4$, the distance from the reflecting surface to the first electric field maximum, to occur as well. Thus, in the experiment, we would expect a background plasma due to delayed ionization with $\lambda/2$, and $\lambda/4$ structures in it due to reflection. Reflection and absorption will also prevent microwave penetration, so we expect to see the plasma disappear behind the front of the ionization. This results in the appearance of motion. This motion may then occur as $\lambda/2$ or $\lambda/4$ jumps, since once these structures develop, the intensity at these points is larger, due to reflection, than the background intensity.

This ionization front motion strongly affects the coupling of microwave energy to the gas. It determines where the energy will be absorbed, since its high density does not allow microwave penetration. Also, since it is moving, it spreads the heating out in the gas. Motion towards the microwave source has been observed by Salisbury and Flint[4], and by Beust and Ford[5]. The velocities were much slower, however, $V \approx 3 \times 10^3$ cm/s for Salisbury and Flint's work, and $V \approx 600$ cm/s for Beust and Ford's work. Raizer[6] advanced a theoretical treatment for the microwave discharge propagation in high pressure air (~1Atm) to explain Beust and Ford's results under CW conditions. Other work by Scharfman, et al[7], observed that for low pressures the breakdown plasma became opaque to microwaves, thus preventing penetration. We have observed the formation of the front, its motion, the prevention of microwave penetration, and measured the plasma density and electron temperature of the front. Good agreement was found between the experiment and the simulation model.

## II. EXPERIMENT

### A. Apparatus

The microwave energy coupling experiments were performed in dry nitrogen using one of the NRL 35 GHz, high power gyrotrons[8]. This gyrotron is capable of 150 kW, 1μsec pulses at 100 pps. The investigation, however, was performed with a microwave power ≈ 112 kW using S polarization. The nitrogen pressure was variable. The data presented is at a pressure of 25 Torr which corresponds to $\nu/\omega \approx 0.65$, where $\nu$ is the collision frequency for electron momentum transfer and $\omega$ is the natural frequency of the microwave radiation. The microwave radiation is introduced into a test chamber using a conical horn with a focusing dielectric lens in front, see Figure 1. The lens has a focal length of 11.2 cm and a diameter of 7.62 cm. The focal spot is elliptical and has an approximate gaussian distribution in intensity with half widths of 1.5 cm and 1.1 cm. The 3dB focal spot area is approximately 1.7 $cm^2$. For 112 kW this implies 33 $kW/cm^2$ average power inside the 3dB spot. Breakdown, without a reflecting surface, was observed to cease at p ≈ 75 Torr for P = 112 kW. Theoretically, we calculate an average power of 27 $kW/cm^2$ is required for breakdown at 75 Torr in nitrogen. This is in reasonable agreement with an estimated intensity of 33 $kW/cm^2$. We have, however, ignored the gaussian spread and assumed an even distribution.

The breakdown experiments were performed with and without a metal surface at the focal point. The planar metal surface could be oriented perpendicular, 90°, or with an angle of 45° to the incident radiation. The metal surface serves to set up a standing wave pattern in front of the surface resulting in 4 $I_o$ at the peaks, where $I_o$ is the intensity of the incident radiation. Also, a thin dielectric could be placed off the metallic surface. This was used in determining the cause of the plasma motion observed and will be discussed later.

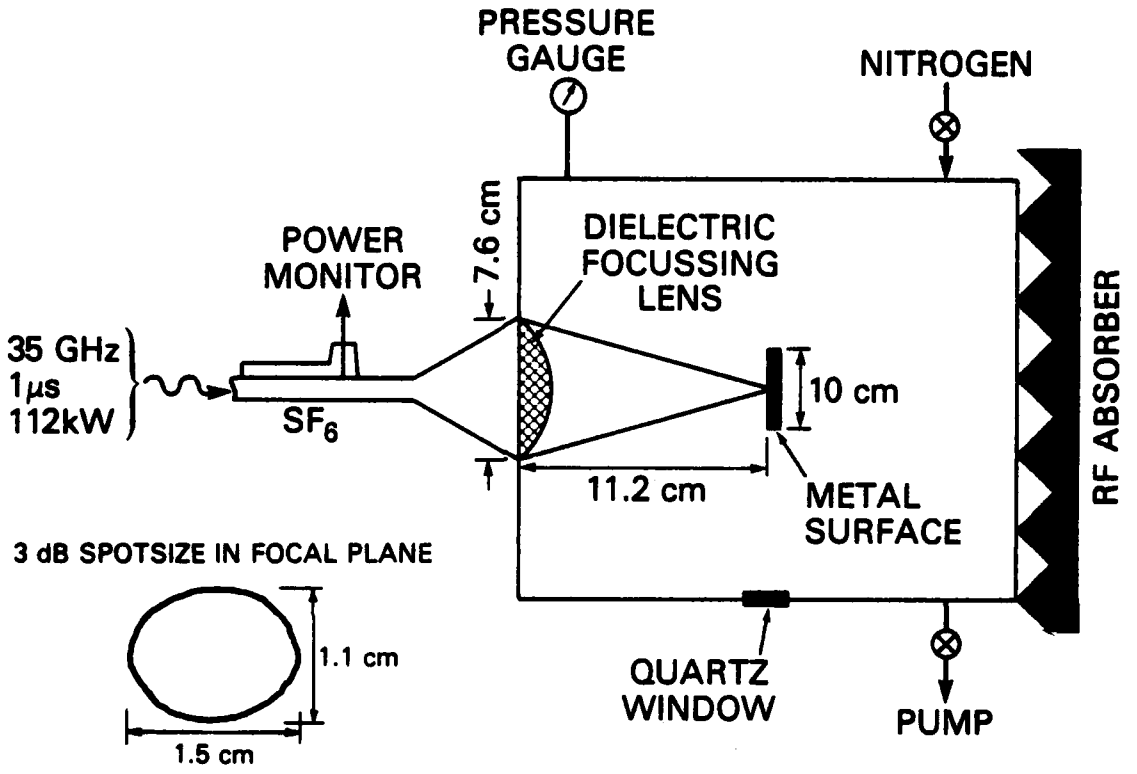


Fig. 1 — Schematic of nitrogen breakdown experiment. Shown as an insert is the 3dB focal spot.

Observation of the plasma was done using a TRW framing/streaking camera. A 20 ns exposure time was used in the framing mode and a 2 μs exposure time in the streaking mode. Due to the amount of light present, multiple exposures were required in order to obtain easily visible photographs. However, some single shot experiments were performed and showed that the results were reproducible shot-to-shot. The electron temperature and density were measured by using a nitrogen-helium gas mixture. In a pure nitrogen mixture, only second positive nitrogen bands were observable. By introducing helium, the 5876Å line could be used with the nitrogen 3371Å band to make the required density and temperature measurements. An Oriel model 7240 monochrometer, f/3.7, with a 10Å bandwidth was used. The monochromator output was measured using a 1P28 photomultiplier with a base modified for nanosecond response time. Absolute intensity calibrations were performed using a calibrated deuterium arc lamp source[9] for 3371Å and a calibrated strip tungsten lamp source[10] for 5876Å.

Our experiments were performed at 25 Torr where we had approximately nine times the intensity required to break down the nitrogen at the focal spot. With the presence of a metal surface, a factor of four reduction in the power required for breakdown occurs due to the standing wave pattern which is set up. Due to the focused nature of the experiment, the standing wave pattern's intensity drops as the distance from the surface is increased. For the 45° target, in fact, there is only a small region of standing waves perpendicular to the surface. It is only for the 90° surface, or the case of a reflective plasma perpendicular to the microwave beam, that a standing wave pattern back the length of the beam line exists. A delayed breakdown from the surface back towards the lens is then expected, since the growth of the plasma is proportional to $e^{tI_o}$. We believe that fluctuations in the reflective plasma surface and UV ionization (if any) will cause a smearing out of the standing wave pattern.

## B. Discussion of the Experimental Results

### 1. Time Resolved Photographs of Breakdown

The observed breakdown patterns for the three cases are shown in Figures 2 through 4. In Figure 2, the breakdown without a surface is shown. A conical plasma is formed with its tail nearest the focal point and head towards the lens. This indicates that a large fraction of the microwave energy is concentrated on axis. For a diffraction limited spot size we calculate the depth of field (where $I = I_o/e$) for our case to be 3.5 cm which is approximately the length of the tail in the early breakdown region observed in Figure 2. The total length of the breakdown region is 5 cm. We calculate a length of 3.7 cm based on incident intensity decreasing to the nitrogen breakdown threshold as we move away from focus. This suggests reflection off the plasma must be occurring. We calculate that ≈ 19% reflection would be required; the simulation suggests $R \leq 28\%$. The breakdown begins at the focal spot, but since the microwave power is above the breakdown threshold, a secondary breakdown region ahead of the focus forms in a time ≈ $2.4 \times 10^{-7}$s after the initial breakdown. As the electron density in this secondary breakdown region increases to $N_c = (\omega^2 + \nu^2)m_e/(4\pi e^2)$, the tail (focus) region disappears due to the microwaves being absorbed and reflected by the plasma at the head. Once the microwave energy is stopped from reaching the plasma in the tail, the plasma temperature there drops rapidly ($\tau \approx 10$ ns), and the emitted light ceases. The plasma itself also begins to decay, but on a longer time scale. Late in time we see that a single absorbing layer about one wavelength thick is formed.

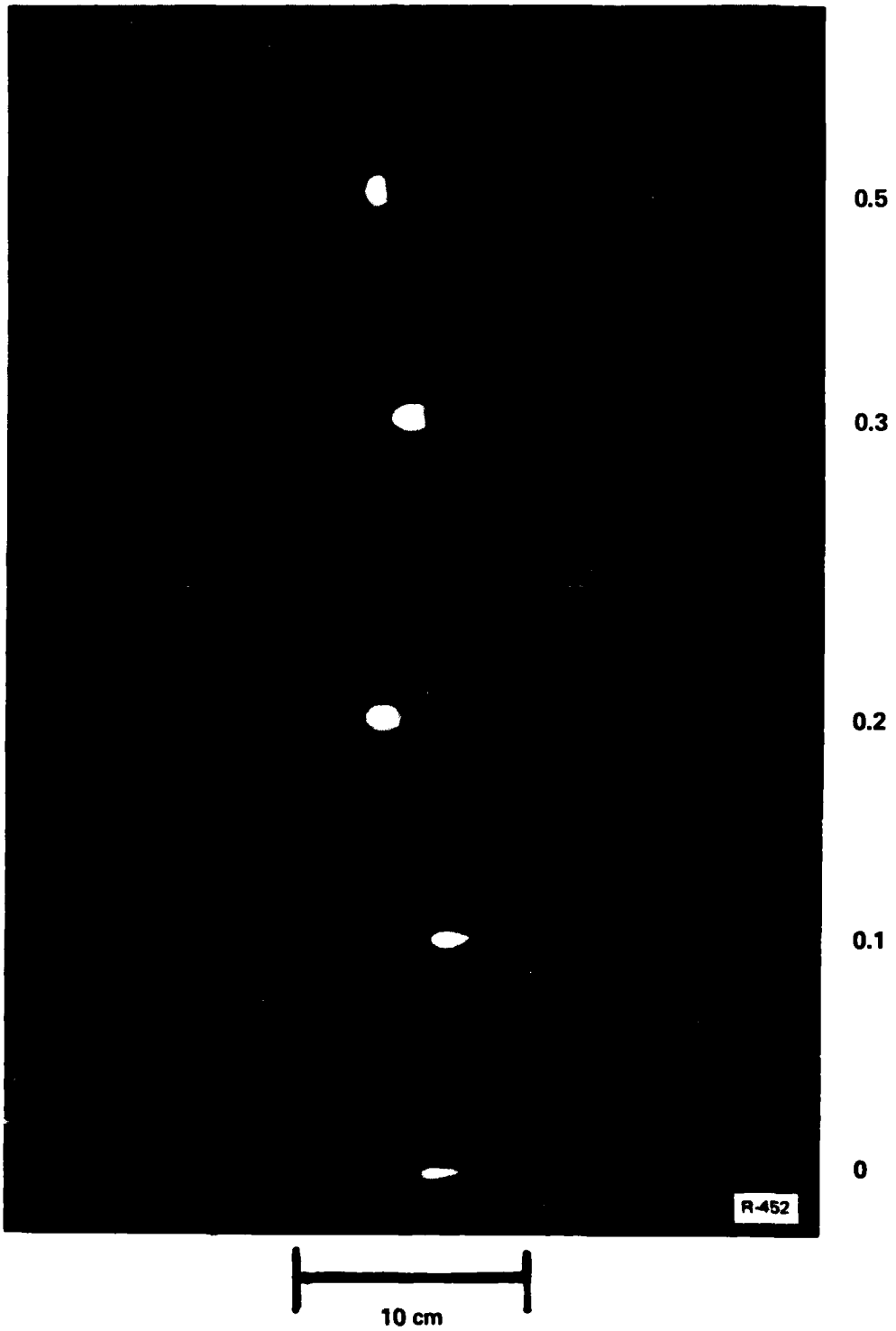


Fig. 2 — Framing photographs of breakdown at 25 Torr $N_2$ for no surface present, $I_o$ = 112 kW or 33 kW/cm$^2$ at focus. The microwaves are incident from the left. Frames are 100 ns apart and have a 20 ns exposure time. Time shown on right refers to the delay after the first observable breakdown and not the microwave pulse.

Figure 3a shows the framing camera data for the perpendicular surface experiment and Figure 3b shows a streak photograph for the same case. We expect a standing wave to be set up off the surface with the first maximum $\lambda/4$ from the surface and with the rest of the maxima spaced $\lambda/2$ apart. This can be seen in Figure 3a. Also observed is a "blooming" of the visible plasma near the target. We believe this is an effect due to the focusing. The microwave beam becomes more intense near focus. Therefore, the diameter of the beam capable of breaking down the plasma increases. Similar to the no target case, an absorbing front travels away from the target towards the microwave source. From the displacement in the streak photograph, we calculate that the plasma moves away from the surface with a velocity $\simeq 4.6 \times 10^6$ cm/s. It continues to move back along the microwave beam until the beam energy decreases sufficiently (due to defocusing) that the beating with any reflected microwaves is below the breakdown threshold. This "stagnation point" is also observed for the 45° surface. Similar behavior is also observed in the computer simulation.

The 45° data is shown in Figure 4. It is similar to the 90° data except fringes occur $\lambda/(2 \cos \theta)$ apart, $\theta = 45°$, with the first fringe at $\lambda/(4 \cos \theta)$ from the surface. Again, an absorbing front moving along the beam axis is observed. This occurs as a result of energy reflected by the plasma along the beam. Since we are far above threshold, we believe a planar plasma, perpendicular to the beam, grows near the target and is initiated by the plasma growth at the standing wave maxima. Its density grows ($N_e \longrightarrow N_c$) and it becomes reflective, setting up standing waves. Plasma density builds at these maxima cutting off microwave penetration, and the process repeats. Visually, this appears as plasma motion. We would expect the motion to jump in either $\lambda/2$ or $\lambda/4$ steps. Some of the 45° data shows $\lambda/2$ bars behind the main moving plasma. In general, however, this is not observed. The $\lambda/2$ spacing is at about the limit of resolution. Further, we believe that fluctuations in the reflective plasma surface cause a smearing out of the standing wave pattern and results in the more solid like appearance we observe for the moving plasma.


**Fig. 3a** — Framing photographs at 25 Torr $N_2$ for 90° metal surface present at focus, $I_o$ = 112 kW. Times shown on right refer to the delay after first observable breakdown.

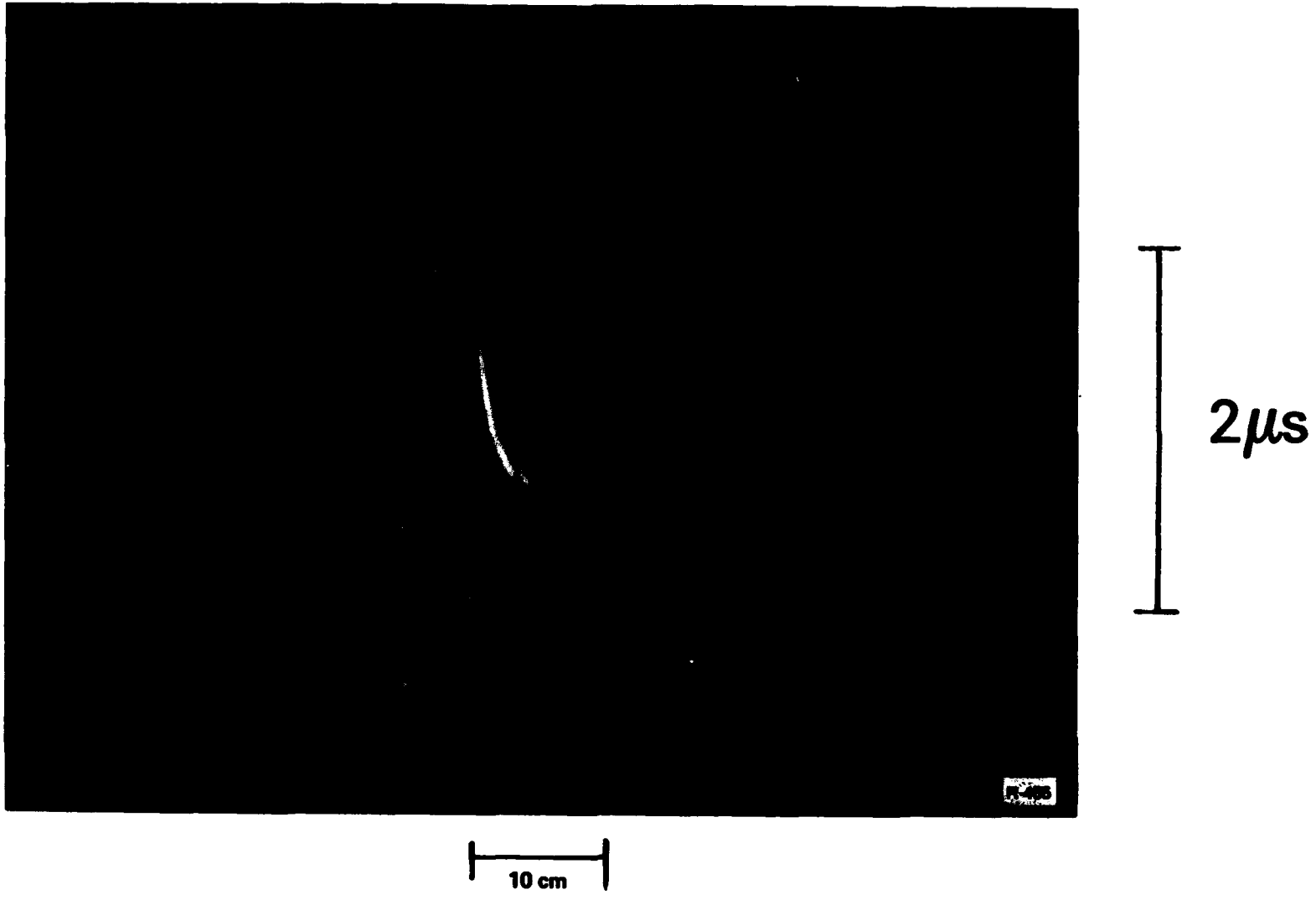


Fig. 3b — Streaking photograph at 25 Torr $N_2$ for 90° metal surface present at focus, $I_o$ = 112 kW. Streaking time was 2 $\mu$s. The velocity of motion for the ionization front is measured to be $4.6 \times 10^6$ cm/s from the photograph.

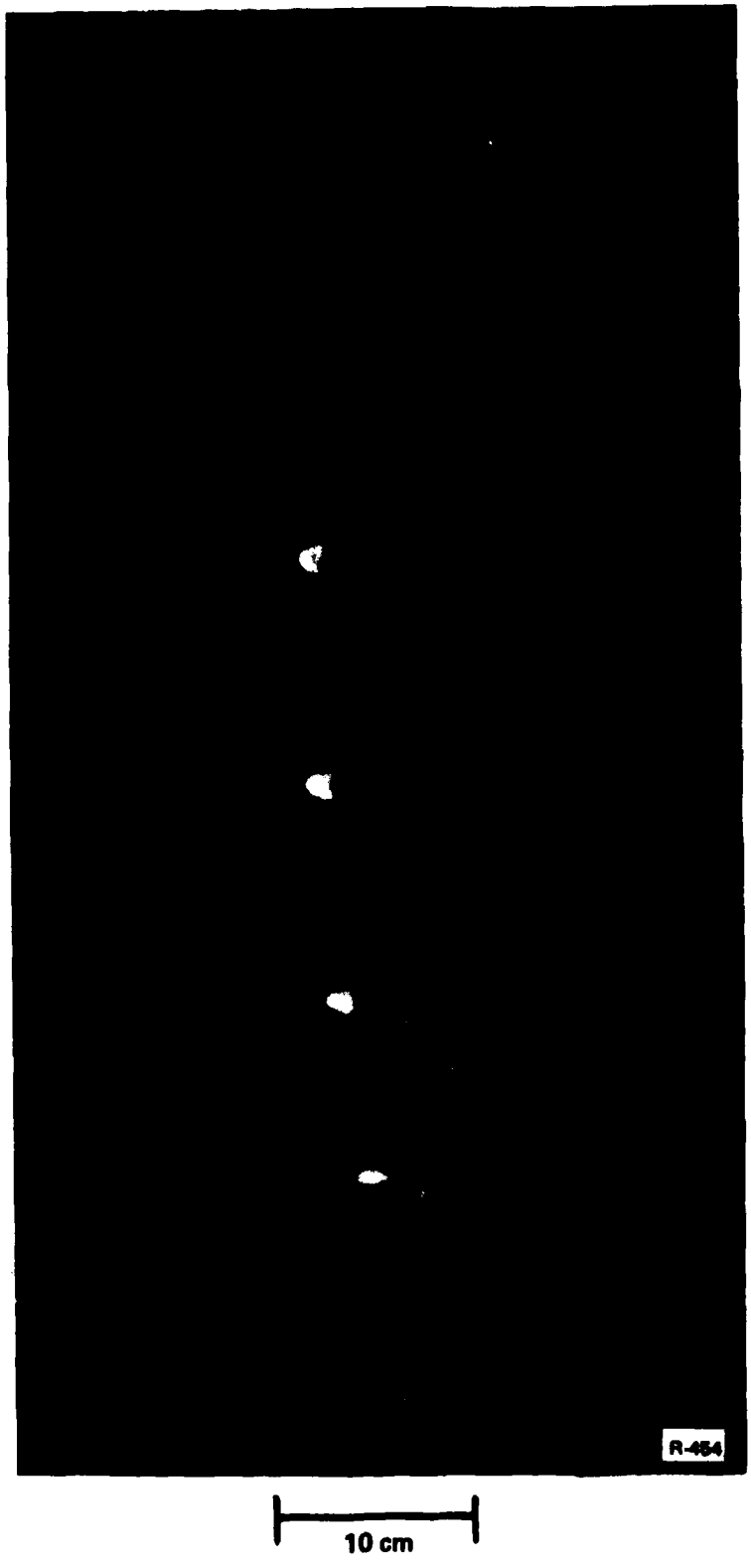


Fig. 4 — Framing photographs at 25 Torr $N_2$ for 45° metal surface, $I_o$ = 112 kW. Times shown on right refer to the delay after the first observable breakdown.

One other possible explanation for the front motion is that UV emission causes ionization to occur in front of the plasma. This new plasma absorbs microwaves, heats up, and then the process repeats. This would result in a uniform smear with no $\lambda/2$ structure. Our data is somewhat suggestive of this. To check this idea we placed a thin dielectric a few wavelengths off the metallic surface to stop UV penetration but allow microwave transmission. If UV ionization was the method of propagation, we expected the plasma to stop moving when it hit the dielectric. The plasma moved through the dielectric barrier. We, therefore, believe the motion to be due to reflection from the plasma itself resulting in ionization fronts. However, ionization due to UV may be responsible for some of the smearing of the $\lambda/2$ and $\lambda/4$ structure. The UV ionization mean free path is $\approx$ 0.05 cm $\ll \lambda/2$ for our conditions.

For the 45° target case the breakdown was examined as the power was decreased. As the power was decreased, the ionization front was observed to stagnate closer and closer to the target, as expected. When the incoming power was 20 kW, $\approx$ 5.9 kW/cm$^2$, we observed only two fringes and no apparent ionization front. At 30 kW the front reappeared. Incident radiation on a metal surface for breakdown to occur at 25 Torr is $\approx$ 0.75 kW/cm$^2$. However, we are only twice the free nitrogen breakdown threshold of 3 kW/cm$^2$, and this will be the dominant threshold for ionization front travel due to delayed ionization.

### 2. Spectroscopic Measurement of Density and Temperature

In order to measure the temperature and density of the electrons, the absolute intensity of the nitrogen second positive band, 3371Å, was compared to the absolute intensity of the neutral helium line at 5876Å. A mixture of the helium and nitrogen was used to perform this experiment. The 3371Å band corresponds to the (0,0) transition in the second positive band system of $N_2$. We obtained the electron temperature from the ratio of the two lines[11] and the electron density from the absolute intensity measurement and the deduced electron temperature.

For an optically thin line and assuming a steady state coronal model, the band intensity at 3371Å can be expressed as:

$$I_{ul} = \frac{N_e \; N_2 \; X_{oc} \; A_{o,o} \; E_{o,o} \; L}{A_o + q \; N_2} \qquad (1)$$

where $N_2$ is the density of the nitrogen molecules in the ground state, $X_{oc}$ is the emission excitation rate coefficient, $A_{o,o}$ is the transition rate for the band at 3371Å and $A_o$ is the total transition rate for the excited state, $E_{o,o}$ is the photon energy, L is the length of the emitting plasma, and q is the quenching rate coefficient of the excited state by the neutral species. A similar equation can be written for the intensity of the helium line. The excitation rate coefficients for 3371Å and 5876Å were obtained using the measured cross sections[12,13] averaged over a Maxwellian electron velocity distribution. The transition rates for 3371Å and for 5876Å are from Refs. (14) and (15) respectively. The quenching rate coefficient[16] for 3371Å by $N_2$ is $1.15 \times 10^{-11}$ $cm^3/sec$.

The measured absolute intensities of 3371Å and 5876Å in a mixture of 15 Torr $N_2$ and 19 Torr He were 28.36 $W/cm^2sr$ and $5.6 \times 10^{-2}$ $W/cm^2sr$. Using the above analysis, we obtain $T_e$ = 3.8 eV and $N_e$ = $4.4 \times 10^{12}$ $cm^{-3}$ for the average density over a 2 cm chord. If quenching of the helium line by nitrogen is included the electron temperature changes slightly, $T_e \approx 4.1$ eV, with a corresponding slight decrease in the calculated electron density. This electron density is in reasonable agreement with Langmuir probe data, $N_e \sim 2 \times 10^{13}$ $cm^{-3}$ and simulation predictions, $N_e = 3.6 \times 10^{13}$ $cm^{-3}$ since these last two are peak local densities. It is reasonable to expect that the peak density is at least four times larger then the average density since the density is proportional to $e^{I_o t}$ and the microwave intensity is gaussian across the chord. (The two centimeter cord is slightly larger then the FWHM of the intensity gaussian.) A comparison of the absolute intensity of the 3371Å nitrogen band for pure $N_2$ as observed experimentally ($I_{exp}$ = $1.12 \times 10^{20}$ $eV/(cm^2\text{-}s\text{-}sr)$) agreed reasonably well with the simulation predictions for similar conditions ($I_{sim} = 3.6 \times 10^{20}$ $eV/(s\text{-}cm^2\text{-}sr)$). As expected, the simulation also predicted a lower electron temperature, $T_e \approx 3.25$ eV, for the pure $N_2$ case.

## III. COMPUTER SIMULATION

The breakdown experiments were modeled neglecting hydrodynamic motion and solving the electric field in spherical geometry[17]. Nitrogen breakdown experiments with no surface, Figure 2, show the microwaves penetrating approximately six wavelengths into the tenuous plasma early in time. The experimental light emission shows the electric field is essentially close to planar for regions near the focal point. However, for distances greater than 4 cm from the focal point, the electric field shows an abrupt transition to a spherical (converging) geometry. The ratio of the inner and outer radius in a spherical system defines an aspect ratio. The converging geometry of the experiment defines an aspect ratio of 3.2 in the converging region and 1.9 in the diffraction limited focal region (approximately planar). We modeled this using an aspect ratio of 2.5 in the simulation. (The simulation has shown that for larger aspect ratios the behavior is similar, but the front does not travel as far.) The simulation used a 0.5μs pulse length, $\tau_p$, at an angular frequency, $\omega$, of $2.2 \times 10^{11}$ $sec^{-1}$ and an average power of 31.25 $kW/cm^2$ at the focal point. The region modeled was three wave lengths long (2.57 cm), had no reflecting surface, and a nitrogen pressure of 25 Torr. This simulation showed ionization front motion similar to that seen experimentally in Figure 2. This is shown in Figure 5 as a time history of the plasma density profile. The electric field drops rapidly beyond the peak electron density $N_e^{max} \approx 3.6 \times 10^{13}$ $cm^{-3}$ and penetrates about one and a half wavelengths into the overdense plasma (Figure 6a). The peak electron and gas temperatures are $T_e \approx 3.5$ eV (Figure 6b) and $T_g \leq 0.027$ eV, respectively. Breakdown simulations with hydrodynamic effects show similar features.

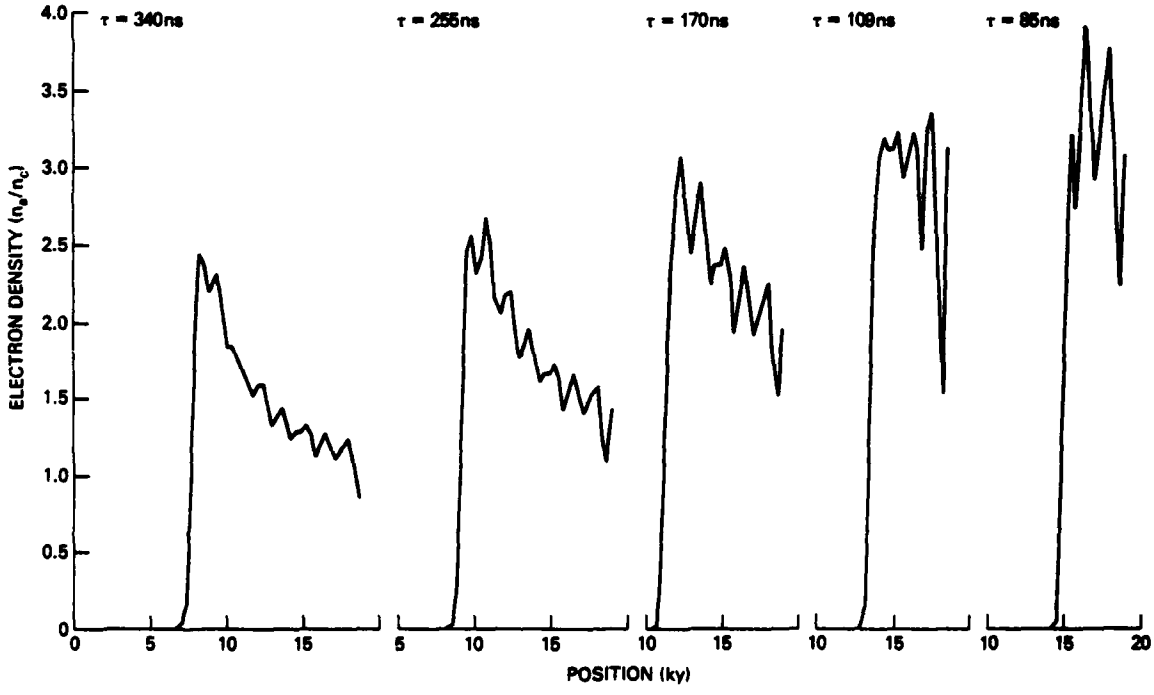


Fig. 5 — Time history of the ionization front in a spherical system. The microwaves are incident from the left with an intensity of 5 kW/cm$^2$. The focused average power is 31.25 kW/cm$^2$ at the right hand boundary. An aspect ratio of 2.5 was used to model the experiment and $N_c$ is the collisionless critical density.

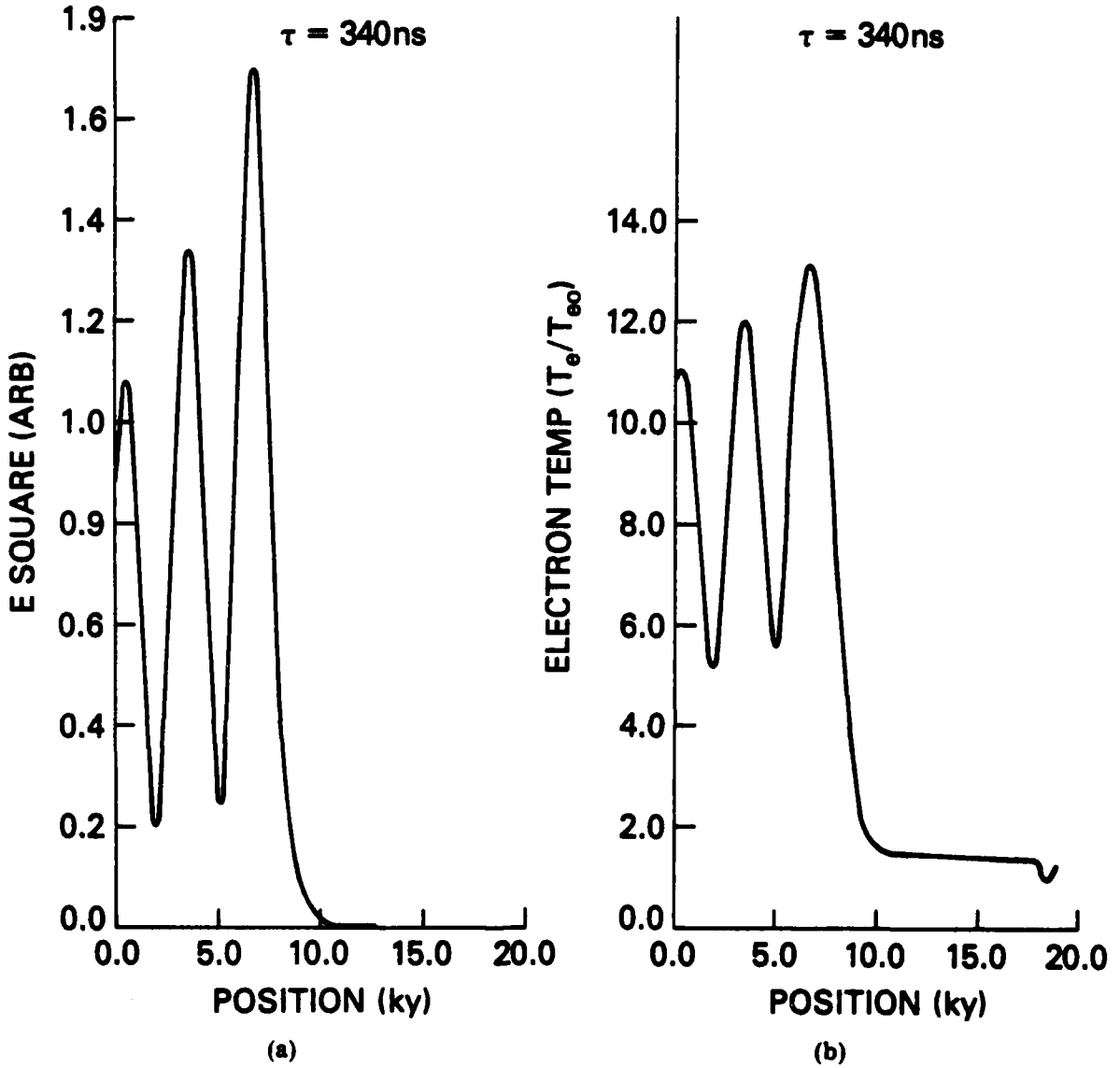


Fig. 6 — (a) Time average intensity for parameters of Fig. 5. Units are in $\alpha = (V_{os}/V_{eo})^2$ such that $\alpha = 1$ corresponds to $I = 9.4$ kW/cm$^2$. (b) Electron temperature for parameters of Fig. 5 where $T_{eo} = 0.25$ eV.

This same simulation was repeated with a reflecting surface at the focal point. Figure 7 shows the simulation results for the electron density. Close to the reflecting surface, the radiation is essentially planar and exhibits the characteristic standing wave pattern. Electron density "pancakes" form at the interference maximum of the electric field. However, at high power the electron density of the pancakes rises to $N_e \geq N_c$ at which time the radiation is partially reflected from the density pancakes. This shifts the breakdown patterns in increments of a quarter-wavelength. The quarter-wavelength fine structure of Figure 8 cannot be resolved experimentally. Similar to the free-nitrogen breakdown, approximately 79% of the incident microwave energy is absorbed. Early in time, the reflecting surface acts to enhance the field. However, once the density rises to absorb the radiation, the field reflects from the density pancakes. Though the reflection was small (R < 28%), the effects of the reflection can also be seen for the no surface simulation in the quarter-wavelength fine structure of Figure 5.

The ionization front is observed to stagnate at about the same position in the experiment with and without a surface. This would only be true if the target is essentially decoupled from the microwave radiation and the absorption efficiencies are approximately equal. The simulations show this to be true with absorption efficiencies of 79% and 72% for breakdown with and without a surface. The simulations predict a front motion of $V \approx 5 \times 10^6$ cm/s early in the pulse and slowing to $2 \times 10^6$ cm/s when the simulation ends in 0.5μs. This gradual slowing of the ionization front is consistent with what is seen experimentally in Figure 3b.

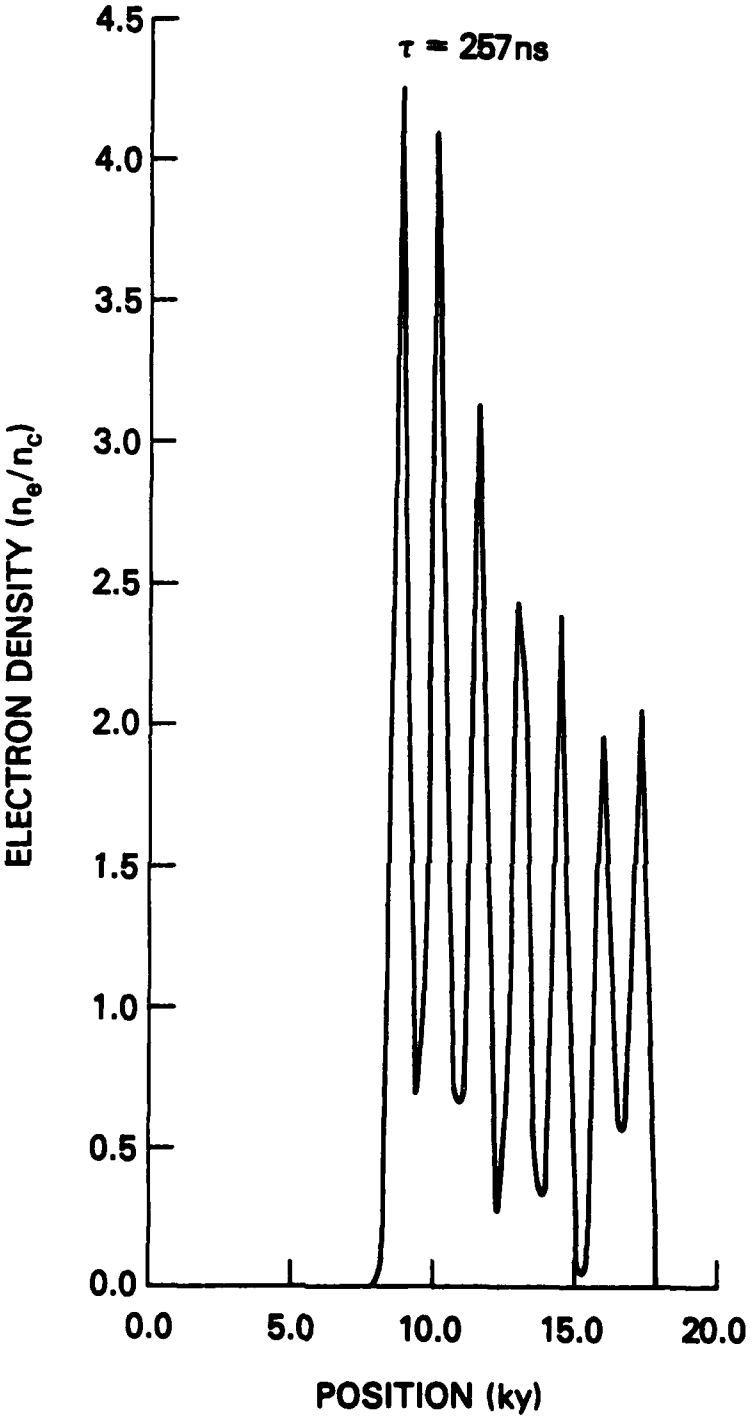


Fig. 7 — Electron density profile at t = 0.26 $\mu$s into the pulse. Same parameters as in Fig. 5 except with a reflecting surface.

## IV. CONCLUSION

In conclusion, we have observed that for $I > I_B$, ionization fronts form and move towards the source at a velocity $\approx 4.6 \times 10^6$ cm/s. These ionization fronts result from both delayed ionization and reflection of microwave energy from the front. The front density can become quite large and is seen to cut-off microwave penetration in about one wavelength in late time. The average chord plasma density was spectroscopically measured to be $N_e = 4.4 \times 10^{12}$ cm$^{-3}$ and the electron temperature to be $T_e = 3.8$ eV for a nitrogen-helium mixture. Langmuir probe measurements of the density gave reasonable agreement with peak densities for pure nitrogen of $N_e \approx 2 \times 10^{13}$ cm$^{-3}$. The cut-off of microwave penetration observed photographically suggests an electron density $N_e = N_c = 2.2 \times 10^{13}$ cm$^{-3}$. We expect the electron temperature in the gas mixture to be higher since $N_2$ vibrational and low lying electronic states act to decrease $T_e$ and monoatomic $H_e$ has no such states. Reasonable agreement was seen with the simulation for the velocity of the ionization front, $N_e$, $T_e$, and $I_{3371}$. The simulation predicts small reflection, $R < 28\%$, and low gas temperature, $T_g \leq 0.027$ eV.

## ACKNOWLEDGMENTS

Some of us (W. Michael Bollen, Mark J. Nagurney, and Michael E. Read) would like to acknowledge many useful discussions with Dr. E. A. McLean and Dr. J. R. Greig on optical diagnostics. We also want to acknowledge Dr. T. J. Wieting and J. L. DeRosa for allowing us to use their microwave chamber and for useful technical discussions. The technical assistance of D. Hardesty was greatly appreciated. This work was supported by Naval Sea System Command under a contract to the Naval Research Laboratory.

## REFERENCES


1. A. D. MacDonald, Microwave Breakdown in Gases, Wiley, New York, (1966).

2. This technique is also used to investigate plasma-enhanced thermal coupling to metal surfaces by T. J. Wieting, J. L. DeRosa and M. E. Read in a parallel program.

3. C. L. Yee and A. W. Ali, "Microwave Energy Deposition, Breakdown and Heating of Nitrogen and Air," NRL Memo Report 4617, (1981).

4. W. W. Salisbury and W. Flynt, "Microwave Energy Coupling Through Re-entry Plasma," Varo, Inc., RADC-TR-64-575, (December, 1964).

5. W. Beust and W. L. Ford, Microwave J., 4(10), p.91, (1961).

6. Y. P. Raizer, Sov Phy JETP, 34, p.114, (1972).

7. W. E. Scharfman, W. C. Taylor, and T. Morita, IEEE-Trans. Antennas Propag., 12, p.709, (1964).

8. M. E. Read, R. M. Gilgenbach, R. Lucey, K. R. Chu, A. T. Drobot, "Spatial and Temporal Coherence of a 35 GHZ Gyromonotron Using the $TE_{01}$ Circular Mode," IEEE Trans. Microwave Theory Tech., 28, p.875, (1980).

9. W. R. Ott, P. Fieffe-Prevost, and W. L. Wiese, Appl. Opt. 12, p.1618, (1973).

10. C. R. Barber, J. Sci. Instrum., 23, p.238, (1946).

11. H. R. Griem, Plasma Spectrostrophy, McGraw-Hill, New York, (1964).

12. M. Imami and W. Brost, J. Chem. Phys., 61, p.1115, (1974).

13. R. M. St. John, F. L. Miller, and C. C. Lin, Phys. Rev. A, 134, p.A888, (1964).

14. R. Nicholls, Ann. Geophys., 20, p.144, (1964).

15. W. L. Wiese, M. Smith, and B. M. Glenn, "Atomic Transition Probabilities," Vol. 1, National Bureau of Standards Reference Data Systems NSRDS-NBS-4, (1966).

16. P. Millet, Y. Salamero, H. Brunet, J. Galy and D. Blanc, J. Chem. Phys., 58, p.5839, (1973).

17. C. L. Yee, A. W. Ali, and W. M. Bollen, "Microwave Energy Coupling in a Nitrogen Breakdown Plasma," NRL Memorandum Report 4869.